

Supplement of Biogeosciences, 11, 6955–6967, 2014  
<http://www.biogeosciences.net/11/6955/2014/>  
doi:10.5194/bg-11-6955-2014-supplement  
© Author(s) 2014. CC Attribution 3.0 License.



*Supplement of*

## **Projected pH reductions by 2100 might put deep North Atlantic biodiversity at risk**

**M. Gehlen et al.**

*Correspondence to:* M. Gehlen ([marion.gehlen@lsce.ipsl.fr](mailto:marion.gehlen@lsce.ipsl.fr))

1  
2 **Projected pH reductions by 2100 might put deep North**  
3 **Atlantic biodiversity at risk.**  
4  
5  
6  
7

8 **Supplement**

9 **Earth system models, model output:** This study draws on standard CMIP5 output from the  
10 Program for Climate Model Diagnosis and Intercomparison  
11 (<http://pcmdi3.llnl.gov/esgcat/home.htm>). It uses models for which three-dimensional pH  
12 fields are available and that were part of a multi-model evaluation (Bopp et al., 2013). The  
13 complete set of RCPs is not available for all models. Individual models have been evaluated  
14 by the respective groups.

15  
16 Table S1. Models used in this study and available RCP per model. References cite key papers  
17 for model validation. Esmfixclim2 = CMIP5 identifier for the simulation referred to as  
18 RCP4.5/fixclim in this study.  
19

model name	available RCPs	piControl (years)	Ref.
CESM1-BGC	4.5, 8.5	500	Hurrell et al. (2013), Long et al. (2013)
GFDL-ESM2G	2.6, 4.5, 6.0, 8.5	500	Dunne et al. (2013)
GFDL-ESM2M	2.6, 4.5, 6.0, 8.5, esmfixclim2	500	Dunne et al. (2013)
IPSL-CM5A-LR	2.6, 4.5, 6.0, 8.5, esmfixclim2	1000	Séférian et al. (2013)
IPSL-CM5A-MR	2.6, 4.5, 8.5	300	Séférian et al. (2013)
MPI-ESM-MR	2.6, 4.5, 8.5	1000	Ilyina et al. (2013)
NorESM1-ME	2.6, 4.5, 6.0, 8.5	252	Tjiputra et al. (2013)

20  
21

1

22 **References**

23

24 Bopp, L. et al.: Multiple stressors of ocean ecosystems in the 21st century: projections with  
25 CMIP5 models, *Biogeosciences*, 10, 6225-6245, doi:10.5194/bg-10-6225-2013, 2013.

26 Dunne, J. P. et al.: GFDL's ESM2 Global Coupled Climate–Carbon Earth System Models. Part  
27 I: Physical Formulation and Baseline Simulation Characteristics. *Journal of Climate* 25:  
28 6646–6665 doi: 10.1175/JCLI-D-11-00560.1, 2013.

29 Hurrell, J. W. et al.: The Community Earth System Model: A Framework for Collaborative  
30 Research. *Bulletin Amer. Meteor. Soc.* 94, 1339-1360, 2013.

31 Ilyina, T. et al.: The global ocean biogeochemistry model HAMOCC: Model architecture and  
32 performance as component of the MPI-earth system model in different CMIP5 experimental  
33 realizations. *Journal of Advances in Modeling Earth Systems*, doi:10.1002/jame.20017, 2013.

34 Séférian, R. et al.: Skill assessment of three earth system models with common marine  
35 biogeochemistry. *Climate Dynamics* 40: 2549–2573 doi:10.1007/s00382-012-1362-8, 2013.

36 Tjiputra, J. F. et al.: Evaluation of the carbon cycle components in the Norwegian Earth System  
37 Model (NorESM). *Geosci. Model. Dev.* 6: 301-325, 2013.

38

39

40

41

42

43

44

45

46

47

48

49

50

51



53 Figure S1: pH of the waters over-lying the seafloor (top) and change in hydrogen ion  
54 concentration corresponding to a decrease in pH of 0.2 units (bottom). pH was calculated  
55 from GLODAP alkalinity and DIC, along with WOA nutrient data. The figure illustrates that  
56 waters having a low initial pH (e.g. deep waters) will experience the largest increase in  $[H^+]$   
57 or acidification for any given decrease in pH. Warm colours indicate high pH, respectively a  
58 low change in  $[H^+]$ .

59

60

61

62

63

64

65

66

67

68

69

70

71

72

73

74

75

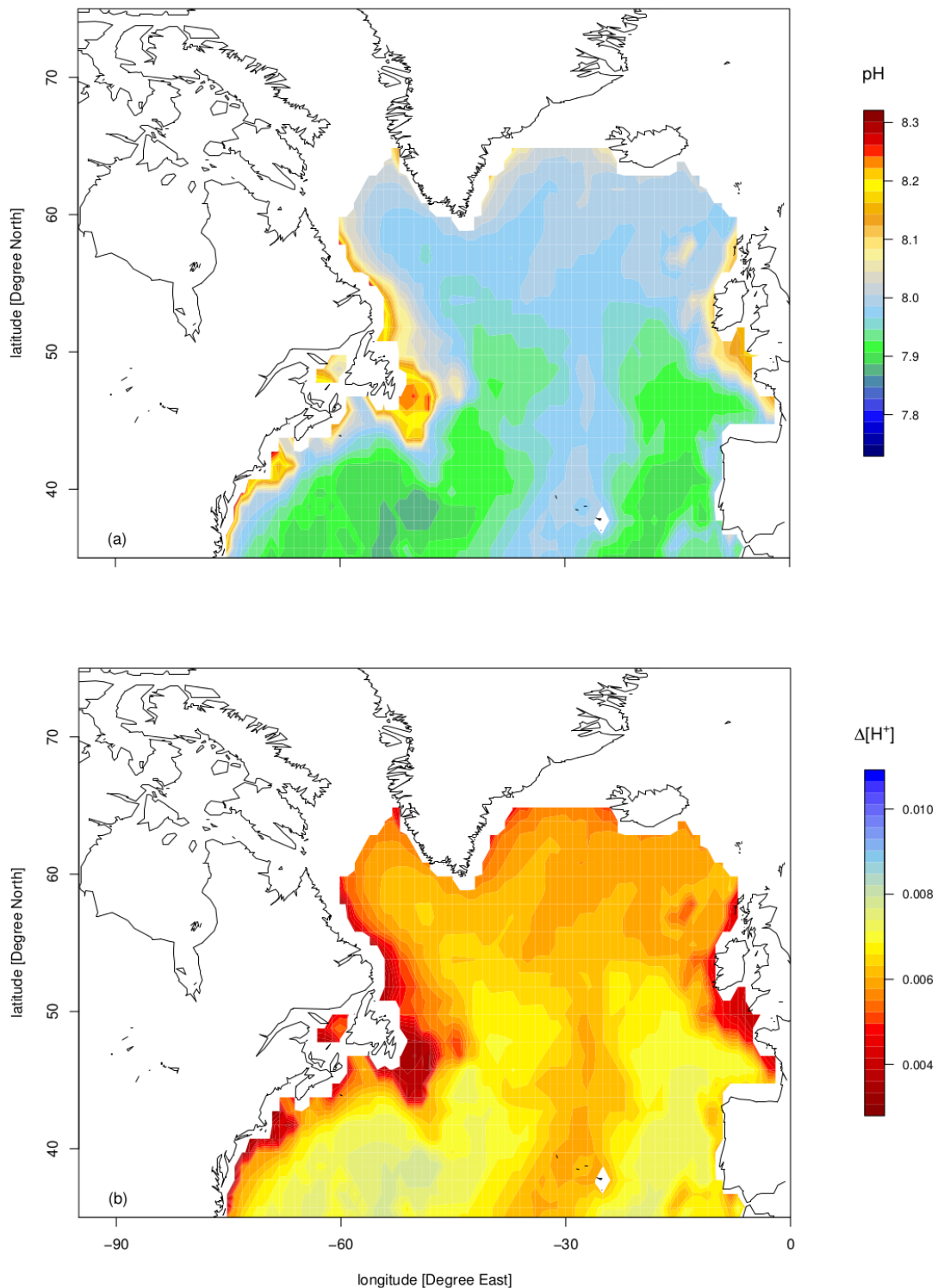
76

77

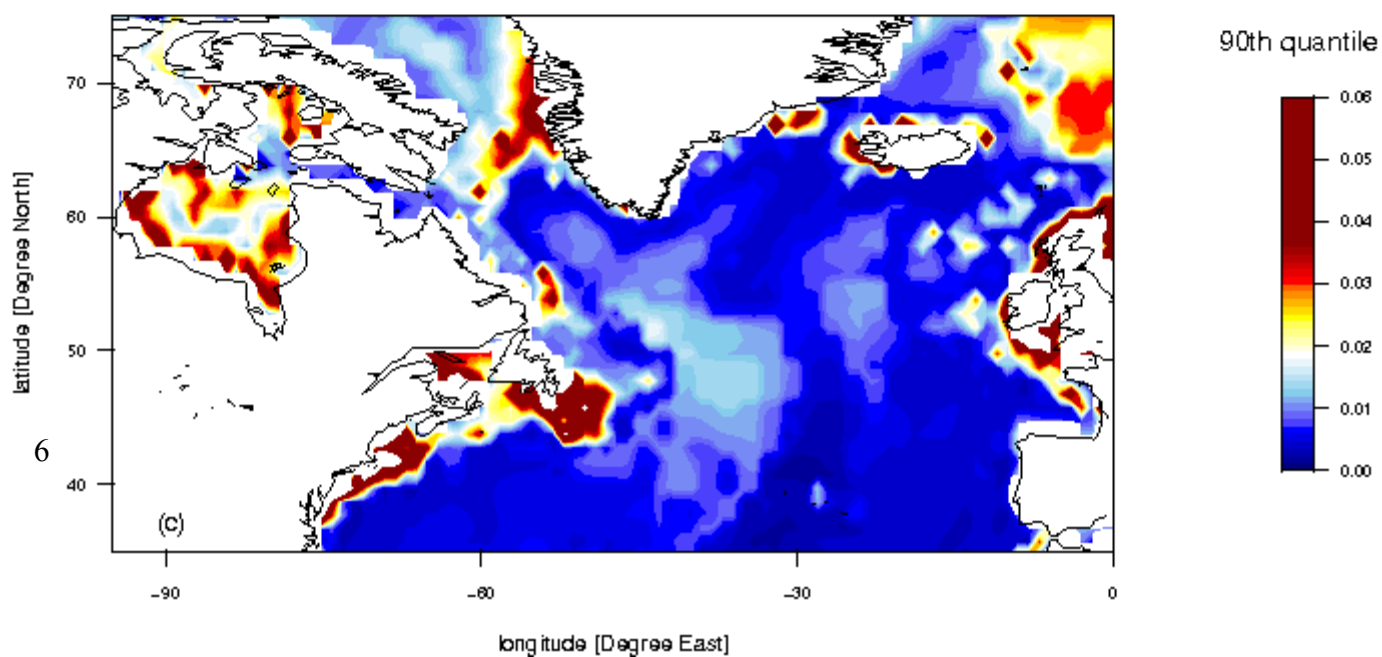
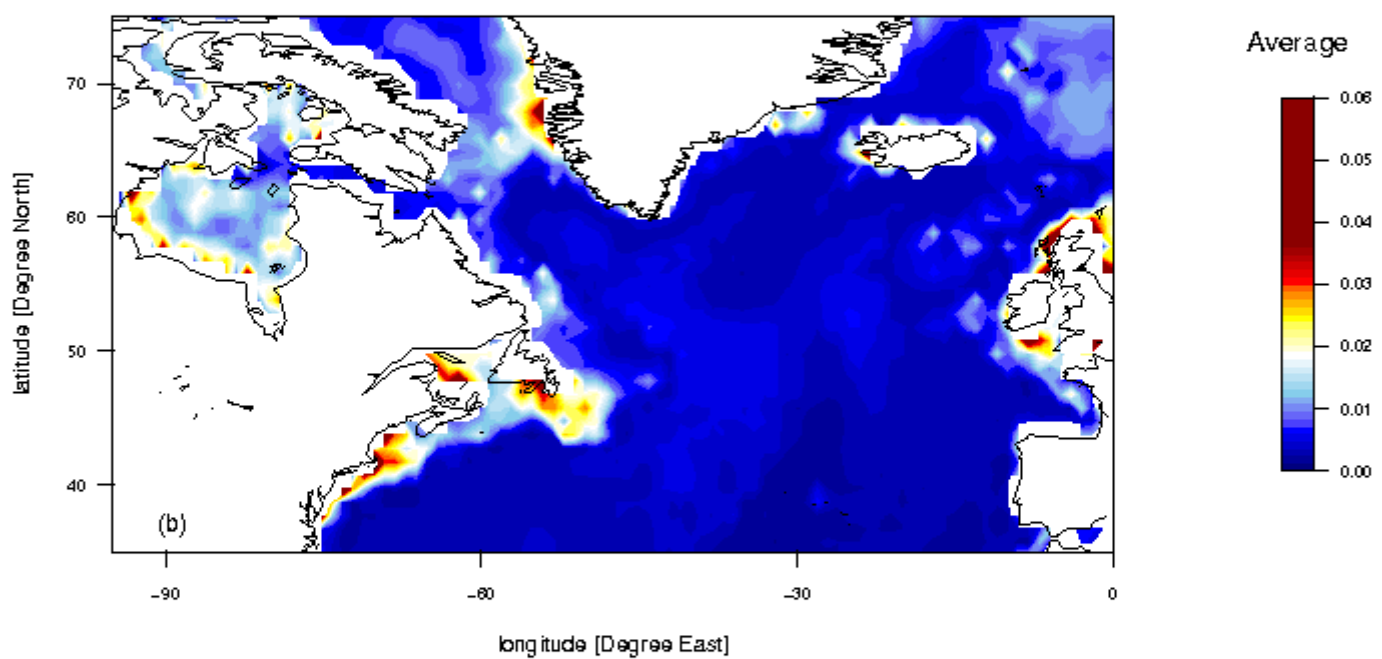
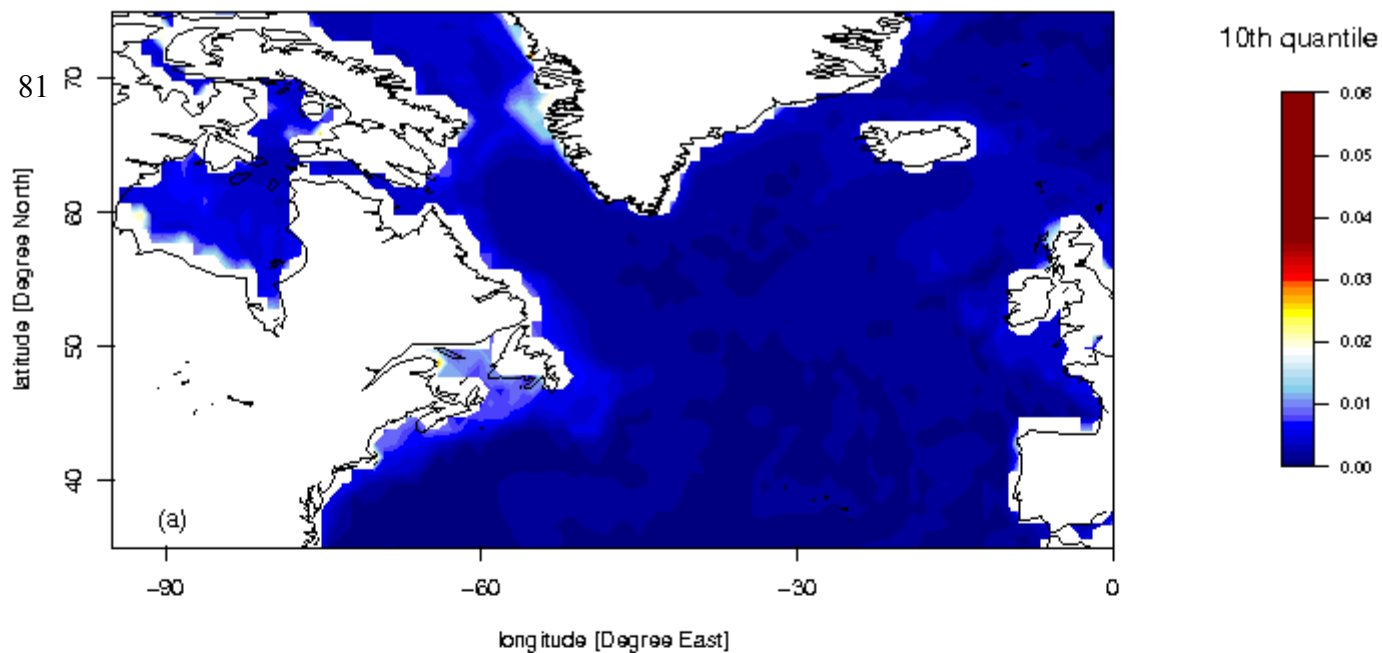
78

79

4



80 Figure S2. Simulated natural variability of deep-water pH from seven Earth system models.  
81 The standard deviation (sdv) of pH is computed for each individual model for the pre-  
82 industrial simulation piControl with the multi-model mean sdv shown on panel (b) and the  
83 multi-model range in sdv as defined by the 10% (a), respectively 90%(c) quantiles.



82 Figure S3. Projected changes in deep ocean pH between pre-industrial and the two IPCC  
83 scenarios RCP2.6 and RCP6.0 by 2100. The panels represent the difference in mean pH  
84 between the pre-industrial and the 2090-2100 average for (a) RCP2.6 and (b) RCP6.0.  
85 Locations of deep-sea canyons and seamounts are indicated as red and black symbols,  
86 respectively. The -0.2 pH contour line is plotted to delineate areas experiencing pH reductions  
87 beyond this threshold.

